SAND2007-7763C

EFFECTS OF STORAGE ENVIRONMENTS ON THE SOLDERABILITY OF NICKEL-PALLADIUM-GOLD FINISH WITH Pb-BASED AND Pb-FREE SOLDERS

Edwin Lopez, Paul Vianco, Samuel Lucero, and Carly George
Sandia National Laboratories[1]
Albuquerque, NM-USA
eplopez@sandia.gov

ABSTRACT
The solderability of a nickel-palladium-gold (Ni-Pd-Au) finish on a Cu substrate was evaluated for the Pb-free solder, 95.5Sn-3.9Ag-0.6 Cu (wt.%, abbreviated Sn-Ag-Cu) and the eutectic 63Sn-37 Pb (Sn-Pb) alloy. The solder temperature was 245ºC. The flux was a rosin-based mildly activated (RMA) solution. The Ni-Pd-Au finish was tested in the as-fabricated condition as well as after exposure to one of the following accelerated storage (shelf life) regiments: (1) 33.6, 67.2, or 336 hours in the Battelle Class 2 flowing gas environment or (2) 5, 16, or 24 hours of steam aging (88ºC, 90%RH). The solderability metrics were the contact angle, θ_C, and the wetting rate, as determined by the meniscometer/wetting balance technique. Auger electron spectroscopy (AES) surface and depth profile analyses were used to assess surface contamination and layer interdiffusion, respectively, as a function of the accelerated test conditions. The Ni-Pd-Au finish significantly improved the solderability of both the Sn-Ag-Cu and Sn-Pb solders by reducing the contact angles when compared to bare Cu. The Battelle Class 2 exposures caused only slight increases of contact angle values for either solder alloy. Exposure to the three steam aging times caused no significant change to the contact angles. The wetting rate of the Sn-Ag-Cu solder decreased only slightly with Battelle Class 2 exposure time. However, the wetting rate of the Sn-Pb solder exhibited a significant drop-off between 33.6 and 67.2 hours, to values similar to those of the Pb-free solder. The steam aging environment did not cause a significant change to the wetting rates of either solder. Exposure to the Battelle Class 2 or steam aging condition brought the low, as-fabricated surface C concentrations to levels commensurate with long-term storage in an air environment. Copper and Fe contaminants were observed on the surface, but at concentrations that were too low to impact solderability. A portion of the Ni layer diffused into the Pd layer to a concentration of 4 at.%. However, Ni diffusion was halted from reaching the Au layer to any appreciable degree by the Au-Pd interface reaction layer. In terms of printed wiring assembly applications, this Ni-Pd-Au finish is particularly well suited for enhancing the solderability of the Pb-free Sn-Ag-Cu alloy. The improved solderability is relatively insensitive to storage time as predicted by either the Battelle Class 2 or steam aging environments, implying that this Ni-Pd-Au finish can provide a relatively wide process window for the Pb-free solders. That process window is only slightly more limited for the Sn-Pb baseline solder.

[1]Sandia is a multi-program laboratory operated by Sandia Corporation, a Lockheed Martin Company, for the United States Department of Energy's National Nuclear Security Administration under Contract DE-AC04-94AL85000.

Key words: Ni-Pd-Au, Storage Environments, Solderability, Pb-free

INTRODUCTION

The transition to Pb-free solders has required that attention be given towards selecting an alternative Pb-free surface finish for printed circuit boards (PCB). Surface finishes must withstand the more severe time-temperature assembly conditions of Pb-free processes as well as support further miniaturize of assembly features and packages. In the high-reliability electronics community (military, space, and satellite applications), there is also the need for PCB finishes to retain adequate solderability over extended storage time that can occur prior to second level assembly. Several Pb-free finishes are currently in use, including electroless nickel immersion gold (ENIG), organic solder preservatives (OSP), immersion silver (Ag), and immersion tin (Sn). However, each of these candidates poses both storage lifetime and assembly challenges as well as solder joint reliability issues. For example, surface finishes that allow the molten solder to contact the copper (Cu) pads and traces – OSP, immersion Ag, and immersion Sn – can result in excessive dissolution of those features. Sulfidation and oxidation of immersion Ag and immersion Sn coatings in the absence of organic inhibitors severely limit the shelf lives of these coatings unless suitable protective measures are put into place. Similar shelf life concerns, as well as long-term reliability issues for small interconnections, have been raised with the ENIG finish.

Alternative PCB finishes that are receiving increased attention are the nickel-palladium (Ni-Pd) and nickel-palladium-gold (Ni-Pd-Au) coatings. These coatings have been used extensively as component lead finishes [1 – 3]. In those applications, the two positive attributes of these finishes are that they are both solderable and wire-bondable, thereby eliminating the need for separate surface finishes

both inside and outside of the component body. The Ni-Pd and Ni-Pd-Au finishes are also receiving renewed attention because of their adaptability to Pb-free soldering applications, particularly as a replacement for the 100% Sn coating that poses a reliability concern with respect to Sn whisker development

The Ni-Pd-Au finish is also being considered as a Pb-free candidate for printed circuit boards (PCBs) [4-7]. Like component lead applications, this coating is suitable for both soldering and wire bonding, the latter capability being particularly suited for chip-on-board assemblies. The Ni and Pd layers may be applied by electroless deposition baths and the Au layer as an immersion finish. Or, all of the layers may be applied by electroplating processes. Most studies on the Ni-Pd-Au PCB finish have examined the electroless type.

The long-term reliability has been demonstrated for solder joints made to Ni-Pd-Au PCB surface finish [8]. However, it is necessary to be mindful of a loss of solder joint strength due to embrittlement. The embrittlement is generally *not* the result of the Au layer as the latter is relatively thin and readily dissolved throughout the solder. Rather, the potential source of embrittlement is the Pd layer. Although the layer is thin, Pd has a slower dissolution rate into the molten solder. A failure to completely dissolve the Pd into the solder bulk can lead to the formation of Pd-Sn intermetallic compound (IMC) particles that "crowd" the solder/Ni interface, leading to a brittle-like fracture behavior by the interconnection. Interestingly, the higher process temperatures associated with Pb-free soldering can reduce the likelihood of this phenomenon.

It is important to understand the roles of the individual Ni, Pd, and Au layers with respect to the wetting and spreading activity of molten solder in order to develop a successful assembly process. A brief background synopsis is provided here. The solderability of a surface is quantitatively measured by the contact angle, θ_C between the molten solder and substrate (coating) surface. Figure 1a illustrates the circumstances that are pertinent to the current study. The smaller the contact angle (θ_C), the better is the solderability performance. The contact angle is determined by the equilibrium balance of three interfacial tensions as expressed by Young's equation:

$$\gamma_{SF} - \gamma_{SL} = \gamma_{LF} \cos\theta_C$$

Equation 1

where γ_{SF} is the solid (substrate)-flux interfacial tension; γ_{SL} is the solid-liquid (solder) interfacial tension, and γ_{LF} is the liquid-flux interfacial tension. All else being equal, a lower interfacial tension, γ_{LF}, reduces the contact angle per Young's equation (1), which contributes significantly to optimum solderability. A lower contact angle is also realized with a larger value of γ_{SF}, which is sensitive to the substrate material and the condition of its surface. Lastly, a reduced value of γ_{SL} will also improve solderability; this parameter is determined primarily by the interface reaction product formed between the molten solder and substrate material.

The wetting and spreading process that underlies the solderability behavior is more complicated in the case of the Ni-Pd-Au finish than it is for a simple copper (Cu) substrate This point is illustrated by the schematic diagram in Fig. 1b. Initially, the solder must wet and spread over the Au layer. Therefore, the Au surface must be contaminant free. A flux will be required to remove the carbon layer that is naturally adsorbed onto Au surfaces. The Au is dissolved into the molten solder. Wetting and spreading continues on the Pd layer. As was the case of the Au layer, the Pd layer must be free of contaminants. The Pd dissolves into the solder, albeit at a considerably slower rate than does the Au layer. Lastly, because the spreading portion of the solderability is largely completed over the Au and Ni layers, the molten solder then needs to only wet to the underlying Ni layer. If the Ni layer is contaminated, dewetting by the molten solder will be observed on the surface. With respect to surface finish terminologies, the Au and Pd layers are the protective finishes – actually, the Pd layer is the primary protective finish – and the Ni layer is the solderable coating. The purpose of the Au layer is to prevent the limited amount of oxidation that can occur on Pd surfaces, which resulted in a slowing of the wetting and spreading rate for the Ni-Pd finishes.

The present study examined the solderability behavior of Ni-Pd-Au finish, all of the layers of which were deposited by electroplating processes. The coating was evaluated in the as-fabricated condition as well as following exposure to Battelle Class 2 or steam-aging accelerated storage environments. The tests were performed with the Pb-free Sn-Ag-Cu alloy as well as with the eutectic Sn-Pb solder. The solderability test used in this study was the meniscometer/wetting balance methodology [9]. This technique captures the height (H) and weight (W) of a solder meniscus, which has risen up the surface of a vertical plate (Fig. 1a), to calculate the value of θ_C. A schematic diagram illustrating those measurements is depicted in Figure 2. The value of θ_C is calculated from the H and W parameters using equation (2) below:

$$\theta_c = \sin^{-1}\left[\frac{4W^2 - \left(\rho g P H^2\right)^2}{4W^2 + \left(\rho g P H^2\right)^2}\right]$$

Equation 2

where ρ is the solder density (gm/cm^3), g is the acceleration due to gravity (cm/sec^2), and P is the sample perimeter (cm). The solder flux interfacial tension, γ_{LF}, can also be independently determined from the experimental data using equation (3):

$$\gamma_{LF} = \frac{\rho g}{4}\left\{\frac{4W^2}{(\rho g P H)^2} + H^2\right\}$$

Equation 3

An analysis of this parameter was not included in the present discussion. In addition to the equilibrium parameters comprising Young's equation (1), the wetting balance test can also provide wetting rate and wetting time data. Shown in Figure 3 is a generalized representation of the plot of meniscus weight as a function of test time. The wetting rate and time to maximum wetting force parameters are shown on the plot. These test procedures have been used to determine the solderability behavior of the eutectic Sn-Pb solder as well as the Pb-free Sn-Ag-Cu alloy on Cu , Au-Ni coated Fe-Ni alloy sheet, and immersion Ag coated Cu substrates, using a variety of fluxes and solder temperatures [10 – 12]. This database provides the means to readily compare performances between different finishes.

EXPERIMENTAL

Substrate Preparation

The test samples were copper coupons that had been coated with a nickel-palladium-gold (Ni-Pd-Au) printed circuit board finish. All of the layers were electroplated coatings. The nominal thicknesses were 10 ± 5 µm (400 ± 200 µin) Ni, followed by 0.1 ± 0.05 µm (4 ±2 µin) Pd, followed by 0.1 ± 0.05 µm (4 ±2 µin) Au. Baseline data were obtained from an earlier study of bare Cu coupons [10]. All of the coupons had the dimensions of 2.54 cm x 2.54 cm x 0.0254 cm and were sheared from rolled sheet stock and flattened to remove any residual curvature. Only the coupons with lateral dimensions to within ±0.013 cm of these nominal values were selected for electroplating and subsequent testing. The Ni-Pd-Au coated copper coupons were subjected to a cleaning procedure that was performed by the supplier at their facility.

Environmental (Aging) Exposure

The Ni-Pd-Au coated samples were exposed to the Battelle Class 2 specification. That environment, which was reproduced in the Facility for Atmospheric Corrosion Testing (FACT) located at Sandia National Laboratories (Albuquerque, NM), is comprised of flowing gas concentrations of 10 ppb H_2S, 200 ppb NO_2, and 10 ppb Cl_2 at 30°C and 70% relative humidity (RH) [13]. These conditions accelerate an exposure to what would otherwise be, a typical indoor, industrial environment. The test coupons were exposed to the Battelle Class 2 conditions for time periods of 0, 33.6 hours, 67.2 hours and 336 hours. These exposure times are approximately equivalent to shelf life storage durations of 12, 24, and 120 months.

A second group of Ni-Pd-Au coated copper coupons were exposed to a steam aging environment per ANSI J-STD-002 (88ºC and 90% relative humidity) [14]. The exposure times were 5, 16 and 24 hours.

Solders and Fluxes

Two solder compositions were studied. The first solder was the Pb-free 95.5Sn-3.9Ag-0.6Cu alloy (wt. %, Sn-Ag-Cu, also designated SAC 396), having a liquidus temperature of 217ºC. The second solder was the 63Sn-37Pb (Sn-Pb) alloy with a eutectic temperature of 183ºC. Solderability testing was performed at 245ºC. The flux was a rosin-based mildly activated (RMA) material that was diluted one-to-one by volume with isopropyl alcohol (IPOH).

Solderability Testing

The meniscus height, H, was evaluated with the meniscometer, which measures the vertical movement of a molten solder meniscus up the side of the coupon by means of a calibrated traveling microscope. The steps of the procedure were as follows: (1) The coupon was coated with a solder flux. (2) The flux was allowed to dry for 10 minutes. (3) The coupon was preheated above the molten solder pot for 20 seconds before immersing the coupon into the solder. (4) The meniscus height, H, was recorded 20 seconds after immersion of the coupon into the solder bath. Five samples were evaluated per each test condition. A mean value for H, along with a standard deviation was calculated from the five tests

The meniscus weight of the solder was measured using the wetting balance. Five separate tests were performed for each condition with this technique, as well. The wetting balance apparatus measures the weight of the rising molten solder meniscus as a function of time. When a coupon is initially immersed into a solder bath, an "upwards" force is

exerted on the sample due to solder displaced by (a) the sample volume and (b) curvature of the molten solder resulting from its surface tension – the "negative meniscus". As wetting takes place, the negative meniscus is lost, and the solder wets and spreads up the sample surface, creating a downward force by its weight. The buoyancy force caused by the displaced solder of the submerged coupon volume is subtracted from the total force to arrive at weight of the meniscus.

Solderability was quantified by the contact angle, θ_C, formed between the liquid solder and the substrate as calculated from equation 2. The error bars were determined by computing the maximum and minimum values of θ_C that resulted from maximum and minimum values of H and W as determined by the mean plus-or-minus one standard deviation of the two respective parameters. A qualitative solderability guideline is depicted in Table 1 [15]. The solder-flux interfacial tension is calculated per equation (3). The error term was computed in a manner similar to that used to determine the error bars of the contact angle. From these values, the difference γ_{SF} - γ_{SL} can also be computed. Prior studies have indicated that contact angles less than 50º as measured by the meniscometer/wetting balance test have corresponded to the successful use of Pb-bearing solders on actual printed wiring assemblies [16 – 19].

Lastly, per Figure 3, a wetting rate and wetting time ("time to W") were calculated from the plots of meniscus weight versus time. The authors have found these parameters, in particular the wetting rate, to be more instructive in terms of the fundamental wetting behavior as opposed to the procedures outlined in industry specifications. It is important to realize at the onset, that the correlation between contact angle and wetting rate or wetting time is not always very strong. Contact angle represents a pseudo-equilibrium condition between the molten solder and the solderable finish (γ_{SL}), in the present case, the Ni layer, as well as between γ_{SF} and γ_{LF} per Young's equation. It is the substrate/flux interfacial tension, γ_{SF} (that is, the condition of the Au surface), which links the contact angle to the condition of the protective Au finish. On the other hand, the wetting rate and wetting time are dependent upon the kinetics of wetting and spreading for the molten solder/flux/substrate system. In the current evaluation, those kinetics are driven largely by the condition of the Au layer (surface and through-thickness) and secondarily, by the intrinsic properties of the Pd layer. It was assumed that the Au layer protected the Pd coating from contamination and/or excessive oxidation.

Five values of each parameter were obtained from the five samples tests per condition. The wetting rate and wetting time parameters were represented by a mean and error term derived from ±one standard deviation.

RESULTS AND DISCUSSION

Contact Angle Performance – Battelle Class 2 Environment

The contact angle data, θ_C, are shown in Figure 4 as a function of Battelle Class 2 aging time for the Ni-Pd-Au coated substrates. The data include the performances of both Sn-Ag-Cu and Sn-Pb solder alloys. The as-fabricated contact angle was 17.1 ±0.4º for the Sn-Ag-Cu solder. The contact angle of Sn-Ag-Cu solder on bare Cu in the as-fabricated condition, that is, without Battelle Class 2 aging was 39 ±1º [10]. Therefore, from the onset, the Ni-Pd-Au finish significantly improved the wetting and spreading performance of the Pb-free Sn-Ag-Cu alloy when compared to bare Cu. As the Battelle Class 2 exposure time increased, the mean contact angle increased slightly to 20.9 ±0.6º after 336 hours. The increase was well within the experimental error, thereby demonstrating the robustness of the Ni-Pd-Au finish to long-term storage.

In the case of the Sn-Pb solder, the contact angle was 3.6 ±1º for the as-fabricated condition. As was the case with the Pb-free Sn-Ag-Cu solder, the Ni-Pd-Au finish improved the solderability of the Sn-Pb solder alloy vis-à-vis bare Cu (unaged, 245°C), the latter case exhibiting a higher contact angle of 13 ±3°. The contact angle increased to 7.4 ±0.3º after 336 hours in the Battelle Class 2 environment. However, the increase was not monotonic. A maximum in the contact angle (11.1 ±0.4º) was observed after 66.7 hours. Nevertheless, all of the contact angle values in Figure 4 remained below that of bare Cu and would assure excellent solderability in printed wiring board assemblies.

The data in Figure 4 showed that the Ni-Pd-Au improved the as-fabricated solderability of both the Pb-free Sn-Ag-Cu and Sn-Pb solders. More importantly, there was no significant degradation to their solderabilities as a function of the Battelle Class 2 exposure of the Ni-Pd-Au finish prior to testing. The maximum that was observed for the Sn-Pb solder at 66.7 hours reflected variability in the Au surface condition as a function of exposure time. Relative to engineering applications, however, the magnitude of those fluctuations were not considered significant.

Contact Angle Performance– Steam Aging Environment

The contact angle data is plotted in Figure 5 as a function of steam aging time for both the Sn-Ag-Cu and Sn-Pb solders. The mean contact angle values of Sn-Ag-Cu solder fluctuated slightly as a function of aging time in the range 14 – 21°, yet still indicating excellent solderability. Although the mean contact angle (17°) after 24 hours was in this range, there was a significant increase in the variability

of the data. Because experimental measurement techniques were ruled out, this trend suggested that 24 hours may have established a benchmark beyond which, there was potentially a fall-off of solderability performance for the Sn-Ag-Cu solder

The Sn-Pb solder exhibited a very similar behavior, albeit, at lower contact angles than were the case for the Sn-Ag-Cu solder. Statistically speaking, there was no significant change to the contact angle after 5 hours and 16 hours of steam aging. The contact angle did exhibit a significant increase after 24 hours, to 9.0 ±0.6°. Although this contact angle value was sufficiently low to indicate excellent solderability, it did suggest that, like the behavior of the Sn-Ag-Cu solder, that there may be a fall-off of solderability for aging times exceeding 24 hours. For both solders, extended steam aging exposure times would be required to confirm this scenario.

A comparison was made between the Battelle Class 2 results (Figure 4) and the steam aging data (Figure 5). Overall there was very little difference between the contact angles of either solder alloy between the two environments. This fact indicated that both aging conditions did not generate significant contamination "agents" on the Au surface to substantially degrade solderability.

Wetting Rate Performance – Battelle Class 2 Environment

The wetting rate, as defined in Figure 3, was evaluated for the Sn-Ag-Cu and Sn-Pb solder alloys after exposure of the Ni-Pd-Au finished samples to the Battelle Class 2 aging treatments. Those data are presented in Figure 6. In the case of the Sn-Ag-Cu solder, the wetting rate values exhibited a slight decrease with exposure time. Recalling Figure 4, the contact angle data exhibited a slight increase with Battelle Class 2 exposure time. Both trends indicated a slight deterioration of overall solderability performance. Per the discussion above, the correlation between the two parameters was linked to slight changes of the Au finish surface with increases to the Battelle Class 2 exposures. More importantly, the overall minimal change to both the wetting rate and contact angle values implied that solderability performance of the Sn-Ag-Cu alloy on the Ni-Pd-Au surface finish will maintain a relatively wide engineering process control window as a function of storage conditions represented by the Battelle Class 2 environments.

The wetting rate of the Sn-Pb solder was considerably faster than that of the Pb-free solder in the as-fabricated condition. However, the Sn-Pb solder exhibited a significant decrease of wetting rate between exposure times of 33.6 hours and 67.2 hours. The wetting rate rebounded slightly after 336 hours, but clearly not to the level of the as-fabricated samples. This behavior was somewhat surprising, given that the Sn-Pb solder is typically exemplary in all aspects of solderability performance when compared to the Pb-free alloys. In terms of developing a root cause for this unexpected behavior, it could only be hypothesized at this point that the minute change to the Au surface caused by the flowing gas mixture slowed the wetting reaction between the Au layer and the Sn-Pb solder. A contributing factor to the increased sensitivity of Sn-Pb solder to the Au surface condition was the reduced quantity of Sn in the alloy. The lower Sn content reduced the driving force for the solder/Au interface reaction, making it more difficult for the molten Sn-Pb solder to "punch-through" the contamination left on the Au by the two longer, Battelle Class 2 exposures.

The contact angle values of the Sn-Pb solder in Figure 4 steadily increased over the same exposure times at which the wetting rate dropped precipitously (0, 33.6, and 66.7 hours). Together, these two trends re-affirmed that there was a change to the Au layer surface through (γ_{SF}) caused by the Battelle Class 2 exposure. When the magnitudes of the changes exhibited by the contact angle and wetting rate were put into the perspective of printed wiring assembly processes, the higher contact angle values would still indicate excellent solderability while the slower wetting rates would only be a concern in fast soldering processes such as the manual or wave soldering of through hole printed circuit boards.

Wetting Rate Performance – Steam Aging Environment

The wetting rate data for the Sn-Ag-Cu and Sn-Pb solder alloys following exposure to the steam aging treatments are shown in Figure 7. Overall, the Pb-free Sn-Ag-Cu solder exhibited wetting rates that were consistently less than those of the Sn-Pb solder, as expected. Otherwise, the two solders exhibited different trends as a function of aging time.

The wetting rate values of the Sn-Ag-Cu solder exhibited a maximum, centered at approximately 16 hours when account was taken of the error bars. A review of Figure 5 showed that the contact angle lacked any statistically significant trend. Therefore, the wetting rate was slightly more sensitive to the condition of the Au surface left behind by steam aging. When consideration was given to the experimental error, data in Figures 5 and 7 would indicate that overall solderability performance of the Sn-Ag-Cu solder would remain more than adequate when using the Ni-Pd-Au finish in actual assembly processes. It should be recognized that the wetting rate of the Sn-Ag-Cu solder, like the contact angle, exhibited wider error bars for the 24 hour exposure. As discussed above, this increased variability suggests that there may be an impending drop-off in wetting and spreading performance for steam aging exposure times that extend beyond 24 hours.

The Sn-Ag-Cu solder wetting rates were compared with those measured on the Ni-Pd-Au surfaces after exposure to the Battelle Class 2 environments (Figure 6). In general, the wetting rates were higher following the steam aging treatments (Figure 6), indicating that the Battelle Class 2 environment was more detrimental towards the wetting and spreading performance than were the steam aging exposures. On the other hand, the range of Sn-Ag-Cu contact angles were nearly the same between the Battelle Class 2 and steam aging treatment exposure times – see Figures 4 and 5. This comparison further substantiated the fact that, although a correlation could be developed between wetting rate and contact angle based on the condition of the Au surface through γ_{SF}, the wetting rate was substantially more sensitive to this Au surface of the Ni-Pd-Au finish than was contact angle for the Sn-Ag-Cu solder.

The mean wetting rate values of the Sn-Pb solder on the steam aged Ni-Pd-Au finish did not show a monotonic trend with exposure time. There was a maximum in the mean wetting rate after the 5 hour exposure, albeit, the difference was not statistically significant. The 16 hour and 24 hour exposure times resulted in wetting rates nearly identical to the as-fabricated condition. A comparison was made of the wetting rate data in Figure 7 (steam aging) with those in Figure 6 (Battelle Class 2 aging). In the latter case, the values representing the as-fabricated and 33.6 hour exposures were similar to those after steam aging. The two data sets differed by the sharp drop-off of wetting rate after the two longer, Battelle Class 2 exposure times (67.2 and 336 hours). The Sn-Pb wetting rate behavior and the contact angle values (Figure 5) were similar in that both parameters were relatively insensitive to the exposure time.

Auger Analysis – Battelle Class 2 Environment

Auger electron spectroscopy (AES) was performed with the objective to correlate solderability behavior (contact angle and wetting rate) with changes to the surface and depth profile chemistry of the Ni-Pd-Au coatings caused by each of the two accelerated aging exposures. The depth profile data are particularly important in order to understand potential interdiffusion between the various layers caused by elevated temperatures and role of interdiffusion, on solderability behavior.

Shown in Figure 8 is the AES data for the Ni-Pd-Au coating in the as-fabricated condition. At the surface, the predominant elements were Au (69 at.%), O (15 at.%), and C (10 at.%). There was 3 at.% of Cu on the surface, which was likely responsible for the elevated O signal due to Cu-O oxide formation. At first glance, the suspected source of Cu would be the substrate material being dissolved into the Au plating bath. However, the application of Ni and Pd preceded the Au plating process and, as such, would serve as barriers to such a mechanism. The depth profile does not indicate that the source of Cu was solid-state diffusion through the layer. Therefore, it can only be surmised that, in fact, the source of Cu was extraneous contamination within the Au layer arising from the plating process.

The primary source of C was the hydrocarbons present in the environment for which, any Au surface is an effective getter material. However, the C levels were relatively low – typical surface C concentrations on Au are 30 – 40 at.%. The Cu levels were not sufficiently high to have interfered with the absorption of C. The concentration of C quickly decreased to zero with depth into the layer, confirming its source as absorption from the environment rather than a homogeneous contamination of the Au layer by the plating chemicals. Although there appeared to be significant intermixing of the Au and Pd layers at their mutual interface, Pd was not recorded within, or on the surface of, the Au layer. Lastly, there were no indications of Ni having solid-state diffused into either the Au or Pd layers.

The AES surface and depth profile analyses were evaluated for the coupons exposed to the Battelle Class 2 environments (Figure 9). The analysis will be limited to the case of the maximum exposure time of 336 hours because it sufficiently represented the other profiles. First, with respect to the minor elements Cu and O, the AES surface analyses showed these to have surface concentrations of: (1) Cu; 2, 5, and 3 at.% and (2) O; 6, 14, and 6 at.% for increasing exposure time. The Cu concentration was similar to that level observed in the as-fabricated condition (Figure 8). The O signal trend correlated with the Cu signal, indicating probable Cu-O oxide formation. The absence of an increasing Cu concentration with exposure time further substantiated the premise that its source was not diffusion from the underlying Cu substrate, but rather metallic contamination of the electroplated Au layer.

A trace of Fe was observed at the surface of the sample exposed for 67.2 hours. The source of Fe is contamination of the plating bath. The fact that it was observed only in this instance implies that the contamination was not widespread in the Au layer. Thus, the Fe contamination would have been of little consequence to the solderability behavior. It is important to note that, based upon the findings of Cu and Fe in the Au layer, it is necessary to tightly control the plating process, not only to obtain the desired thicknesses but, also, when depositing such thin layers, to minimize contamination levels in the plating baths. Those contaminants will be deposited with the individual Ni, Pd, or Au layers.

The extent of C present on the surface increased with exposure time and then leveled off at the maximum duration. Specifically, the C concentrations went from an as-fabricated value of 10 at.% to 15, 30, and 26 at.% for 33.6, 67.2, and 336 hours, respectively. The latter C concentration values of 30 and 26 at.% were commensurate with those observed on Au surfaces with nominal storage times in air. Therefore, the low value of the as-fabricated sample suggested that the coupons simply experienced minimal exposure to the environment.

The interdiffusion behaviors of Au, Pd, and Ni elements were of particular interest in the AES depth profiles. The Pd did not diffuse to the surface of the Au and was not present within the Au layer after the 33.6 hour exposure. Palladium was observed at a trace level of 0.1 at.% on the surface, and concentrations of 0.1 – 0.2 at.% within the Au layer after the two longest aging times of 67.2 hours and 336 hours. None was detected at either location after 33.6 hours.

The behavior of Ni was analyzed in a similar fashion. Nickel was absent from the surface after the 33.6 hour exposure time, but then present in trace concentrations of 0.6 at.% and 0.3 at.% after 67.2 hours and 336 hours, respectively. Within the Au layer, Ni was not present after 33.6 hours, but was then observed at concentrations of 0.2 – 0.3 at.% and 0.1 – 0.5 at.% after 67.2 hours and 336 hours, respectively, accompanying the Pd signal as described above.

The most interesting observation made from Figure 9 was that the Ni had diffused into the Pd layer. The Ni concentration levels within the Pd layer were independent of the exposure time, showing a gradient of
4 – 0 at.% from the Ni-Pd interface to the Au-Pd interface. The Ni diffusion was stopped by the Au-Pd diffusion zone that had formed at the latter interface. The zone size, itself, did not change as a function of Battelle Class 2 exposure time. It is well established that Ni would have readily diffused through the Au layer at even these moderately high temperatures and would have readily reached the surface given the very limited Au thickness. Instead, only a trace amount of Ni (0.25 at.%) was recorded at the Au layer surface, indicating that, under the three exposure times and at a temperature of 30°C, the Ni solid-state diffusion had been largely halted by the Au-Pd reaction zone, causing Ni to become saturated within the Pd layer[1].

[1] This characteristic of one-direction diffusion, together with low concentration of Ni in the Pd layer, were not expected given that both elements form a solid solution over the entire binary composition range.

Additional analysis can now be compiled with respect to Pd and Ni concentrations at the surface and within the Au layer. It was observed above that Pd did not diffuse into Ni layer. Rather, the Ni diffused into the Pd layer. Therefore, it was surmised that the trace amounts Pd found in the Au layer and on the surface provided a conduit by which, the trace amounts of Ni were similarly associated with the Au layer. The traces of Pd and Ni that were observed at the surface and within the Au layer were not accompanied by an O signal. Therefore, the Au layer protected the Ni and Pd within it, as well as Ni within the Pd layer, from oxidation, thereby minimizing any risk of degradation to the wetting and spreading of either molten solders during dissolution of the Au and Pd layers.

As an interim summary, the AES analyses indicated that exposure to the Battelle Class 2 environments caused the following changes: (1) the surface concentration of C rose to levels typically observed of Au surface after long-term exposure to the ambient atmosphere; (2) trace concentrations of Cu, Ni, and Pd were observed at the surface that were in an oxidized state; and (3) despite the diffusion of Ni into the Pd layer and the trace amounts of Pd and Ni in the Au layer, neither phenomenon showed oxidation of the diffused species. Lastly, it was also evident that the Au layer surface did not react with the S, N, or Cl components in the Battelle Class 2 environment.
The three listed phenomena were not of such magnitudes that they resulted in an obvious, severe deterioration of Ni-Pd-Au solderability. Thus, smaller effects were considered by comparing AES depth profile analysis to the contact angle data in Figure 4 and wetting rate data in Figure 6. In the case of contact angle (Figure 4), it was assumed that the contact angle was affected by the surface condition of the Au layer caused by the C build-up as the latter affected γ_{SF}. Also, the presence of the Ni-Pd interdiffusion layer could have potentially altered γ_{SL}. The absence of oxidation of the interdiffused Ni and Pd elements as well as oxidation of the Ni solderable layer would have minimized any effect on the contact angle. Also, the Ni content of the Pd layer remained relatively limited at 4 at.%. In both cases, the absence of a strong, consistent dependence upon the exposure time for either solder tends to rule out the Ni-Pd interdiffusion phenomenon as a critical factor in the solderability performance. Thus, the primary effect was most likely the C contamination of the Au surface and the efficacy of the flux to remove that contamination. When a distinction is made between the Sn-Ag-Cu and Sn-Pb solders, the latter was more sensitive to the Au surface condition caused by the Battelle Class 2 exposure.

A similar conclusion was drawn when comparing the AES analyses and wetting rate data (Figure 6). The sensitivity of the Sn-Pb wetting rate could be correlated most strongly to

the C contamination on the Au surface. (The wetting rate was more sensitive to the C surface concentration than was contact angle.) In the case of the Sn-Ag-Cu alloy, the wetting rate showed the same insensitivity to any aspects of the surface or interdiffusion conditions resulting from the Battelle Class 2 exposures.

Auger Analysis – Steam Aging Environment

The AES surface and depth profile analyses were used to evaluate the Ni-Pd-Au finish exposed to the steam aging treatment. The surface and depth profile evaluations were very similar between all three exposure times: 5, 16, and 24 hours. Therefore, the steam aging effects will be discussed with reference to the data from the sample exposed to 16 hours. The AES depth profiles are shown in Figure 10 for two scales. The plot in Figure 10a shows the elemental distributions at the longer scale into the Ni layer resulting from sputtering for up to 15 min. The plot in Figure 10b shows a contracted scale of the depth profile in order for the data to coincide with Figures 8 and 9 for comparison purposes.

The C concentration on the Au surface remained relatively constant at 27, 19, and 27 at.% for 5, 16, and 24 hour exposures, respectively. In all cases, the concentration of C quickly decreased to zero. Trace concentrations of Cu were observed on the surface, having values between 0 – 2 at.%, but with no particular dependence on aging time. A surface Fe concentration of 2 at.% was observed, but only after the 24 hour exposure. As was the case with C, the Cu and Fe levels dropped quickly to zero with small penetration into the Au layer.

The Ni and Pd elements were present at trace levels of < 1 at.% at the surface, and within the Au layer. The Pd surface concentrations were less than 0.2 at.% for all cases and the Ni concentrations were 0.75, 0.93, and 0.86 at.% after 5, 16, and 24 hours. Within the Au layer, the concentrations of Pd and Ni remained less than 0.6 at.% for all treatments with no expressed dependence on aging time nor any indication of their having been oxidized. At these concentrations, it was not likely that separately, or together, the Ni and Pd levels would have severely degraded the solderability performance of the molten Sn-Ag-Cu or Sn-Pb alloys.

As was observed after exposure to the Battelle Class 2 environments, Ni had diffused through the Pd layer, being stopped by the Au-Pd interface reaction zone. The Ni concentration ranged from 4 at.% to 0 at.% from the Ni-Pd interface to the Au-Pd reaction zone. There was no diffusion of Pd into the Ni layer. Similar characteristics pertained to the other two aging times (5 and 24 hours), as well.

A comparison was made between the AES analyses of the Battelle Class 2 aged samples versus those exposed to the steam aging treatment. The steam aging regiment was responsible for slightly higher surface concentrations of C, Cu, Pd, Ni, O, and Fe. On the other hand, the characteristics of interdiffusion of Ni into the Pd layer were very similar between the two environmental conditions. Two scenarios can be construed to have caused the similar depth profiles. First, as a thermally activated process, the combination of time and temperature for the two processes caused equivalent diffusion behavior of Ni into Pd. Or, secondly, the diffusion process had reached equilibrium under the milder Battelle Class 2 conditions; thus, no further diffusion took place under the harsher time/temperature conditions of the steam aging regiment.

Lastly, the contact angle data (Figure 5) and wetting rate results (Figure 7) were compared with the AES surface and depth profile results. There was an absence of a strong dependence of contact angle on exposure time exhibited by either solder alloy. The wetting rate data of the Sn-Ag-Cu solder showed a slight trend versus exposure time. However, that trend was not monotonic; rather, the wetting rate exhibited a *maximum* at 16 hours. There was no significant trend for the Sn-Pb solder. Therefore, the elemental absorption and diffusion processes revealed by AES surface and depth profile analyses, which revealed, specifically, surface contamination effects by C, Cu, O, Fe, Ni, and Pd, as well the Ni-Pd interdiffusion process, had a very minimal effect on the solderabilities of the Ni-Pd-Au finish by either Sn-Ag-Cu or Sn-Pb solders.

SUMMARY

1. The solderability of a nickel-palladium-gold (Ni-Pd-Au) finish on a Cu substrate was evaluated for the Pb-free solder, 95.5Sn-3.9Ag-0.6Cu (wt.%, abbreviated Sn-Ag-Cu) and the eutectic 63Sn-37Pb (Sn-Pb) alloy. The solder temperature was 245ºC. The flux was a rosin-based mildly activated (RMA) solution. The Ni-Pd-Au finish was tested in the as-fabricated condition as well as after one of the following accelerated storage (shelf life) regiments: (1) 33.6, 67.2, and 336 hour exposures in a Battelle Class 2 flowing gas environment or (2) 5, 16, and 24 hours steam aging (88ºC, 90%RH). The solderability metrics were the contact angle, θ_C, and the wetting rate, as determined by the meniscometer/wetting balance technique. Auger electron spectroscopy (AES) surface and depth profile analyses were used to assess surface contamination and layer interdiffusion processes, respectively, as a function of the accelerated test conditions.

2. The Ni-Pd-Au finish significantly improved the solderability of both the Sn-Ag-Cu and Sn-Pb solders when compared to bare Cu. The Battelle Class 2 exposures caused only slight increases of contact angle values for either solder alloy. Exposure to the three steam aging times caused no significant change to the contact angles from the as-fabricated values.
3. The wetting rate of the Sn-Ag-Cu solder decreased only slightly with Battelle Class 2 exposure time. However, the wetting rate of the Sn-Pb solder exhibited a significant drop-off between 33.6 and 67.2 hours, to values similar to those of the Pb-free solder. The steam aging environment did not cause any significant change to the wetting rates of either solder as a function of the exposure time.
4. The AES surface analyses showed the as-fabricated Au layer to have a relatively low carbon (C) contamination level. There was no intrinsic C contamination within any of the layers. Exposure to the Battelle Class 2 or steam aging condition brought the surface C concentrations to levels commensurate with long-term storage in an air environment. Copper and Fe contaminants were observed on the surface, but at concentrations that were too low to impact solderability. The Ni was observed to interdiffuse into the Pd layer to a concentration of 4 at.%. However, Ni diffusion was halted from reaching the Au layer or its surface to an appreciable degree by the Au-Pd interface reaction layer.
5. In terms of engineering applications for printed wiring assemblies, this Ni-Pd-Au finish is particularly well suited for enhancing the solderability of the Pb-free Sn-Ag-Cu alloy. The improved solderability is relatively insensitive to storage time as predicted by either the Battelle Class 2 or steam aging environments, implying that the Ni-Pd-Au finish can provide a relatively wide process window for the Pb-free solders.

ACKNOWLEDGEMENTS

The authors wish to thank Bill Wallace of Sandia National Labs for the Auger Electron Spectroscopy analysis. The authors are also grateful to Don Susan of Sandia National Labs for his careful review of the manuscript. The authors also extend their appreciation to Kurt Summa, of FTG Corporation, for providing the plated samples for testing.

REFERENCES

1. P. Vianco, "An Overview of Surface Finishes and Their Role in Printed Circuit Board Solderability and Solder Joint Performance", *Circuit World* **25** (1998) pp. 6 – 24.
2. D. Romm and D. Abbott, "Steam-Age Evaluation of Ni/Pd Lead Finish," *Surface Mount Technology* January 1999, pp. 86 – 91.
3. D. Romm, D. Abbott, and B. Lange, "Shelf-Life Evaluation of Nickel/Palladium Lead Finish for Integrated Circuits", Texas Instruments Report dated April, 1998 (SZZA002)
4. D. Yee, "The Use of Electroless Nickel, Electroless Palladium, Immersion Gold on PCB and IC Packages, Rohm and Hass Electronic Materials HTML site, April 2007.
5. Z. Mei and A. Eslambolchi, "Evaluation of Ni/Pd/Au as an Alternative Metal Finish on PCB," *Circuit World* 22/2 (1999) pp. 18 – 26.
6. K. Banerji and E. Bradley," Manufacturability and Reliability of Products Assembled with New PCB Finishes," *Proc. Surface Mount Inter. Conf.* (SMTA, Edina, MN; 1994) p. 584.
7. F. Houghton, "Alternative Metallic Finishes for PWB – An ITRI/October Project", *Proc. IPC Expo* (IPC, Northbrook, IL; 1997) p. S16-4-1.
8. R. Johnson, V. Wang, and M. Palmer, "Thermal Cycle Reliability of Solder Joints to Alternative Plating Finishes," *Proc Surface Mount International* (SMTA, Edina, NM; 1998).
9. P. Vianco, "An Overview of the Meniscometer/Wetting Balance Technique for Wettability Measurements," *The Metal Science of Joining* eds. M. Cieslak, et al., (TMS, Warrendale, PA: 1992), pp. 265 – 284.
10. E. Lopez, P. Vianco, and J. Rejent, "Solderability Testing of 95.5Sn-3.5Ag-0.6Cu Solder on Oxygen-Free High-Conductivity Copper and Au-Ni-Kovar, "*J. Electronic Mater.* 32 (2003), pp. 254 – 260.
11. E. Lopez, P. Vianco, R. Buttry, S. Lucero, and J. Rejent, "Effects of Storage Environments on the Solderability of Immersion Silver Board Finishes with Pb-Based and Pb-free Solders," *Proc. Pan Pacific Conference* (SMTA, Edina, MN; 2005), CD ROM.
12. E. Lopez, P. Vianco, S. Lucero, and R. Buttry, "Comparison of the Solderability Performances of Inhibitor Containing and Inhibitor Free Immersion Silver Coatings," *Proc. Pan Pacific Conference* (SMTA, Edina, MN; 2007), CD ROM
13. C. J. Greenholt, N. R. Sorensen, G. A. Poulter, T.R. Guilinger, "Characterization of the Facility for Atmospheric Corrosion Testing (FACT) At Sandia" *Sandia Report* SAND92-1864 (Sandia National Laboratories, Albuquerque, NM; 1992).
14. IPC/EIA/JEDEC J-STD-002B, Joint Industry Standard "Solderability Tests for Component

Leads, Terminations, Lugs, Terminals and Wires", American National Standard Institute (February 2003).
15. R. J. Klein, Wassink, Soldering Electronics, (Ayr. Scotland: Electrochemical Publications Limited, 1984) p. 235.
16. A. Jackson, I. Artaki, and P.Vianco, "Manufacturing Feasibility of Several Lead Free Solders for Electronic Assembly," *Proc. 7th Inter. SAMPE Electronics Conf.* (Parsippany, NJ; June 21, 1994), p. 381.
17. I. Artaki, A. Jackson, and P. Vianco, "Fine Pitch Surface Mount Assembly with Lead-Free, Low Residue Solder Paste," *Proc. Surface Mount Inter.,* (San Jose, CA Aug. 28, 1994), p. 495.
18. P. Vianco, J. Rejent, I. Artaki, and U. Ray, "An Evaluation of Prototype Circuit Boards Assembled with a Sn-Ag-Bi Solder," *Proc. IPC Works '99* (IPC, Northbrook, IL; 1999), p. S-03-3-1.
19. P. Vianco and A. Claghorn, "Effect of Substrate Preheating on Solderability Performance as a Guideline for Assembly Development – Part I: Baseline Analysis," *Soldering and Surface Mount Technology* No. 24 (1996) p. 12.

Table 1 - "Relative Wettability Guideline" Using Contact Angle (θ_C) As "General" Metric

Contact Angle (θ_C) Range	Relative Wettability
$0^o < 0 < 10^o$	Perfect
$10^o < 0 < 20^o$	Excellent
$20^o < 0 < 30^o$	Very Good
$30^o < 0 < 40^o$	Good
$40^o < 0 < 50^o$	Adequate
$55^o < 0 < 70^o$	Poor

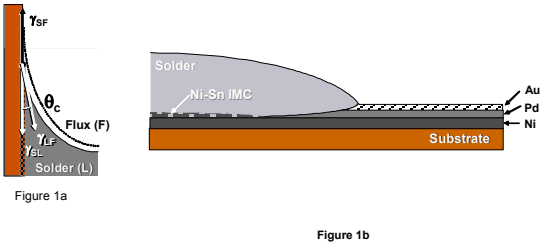

Figure 1a

Figure 1b

Figure 1 – (a) Equilibrium balance of the three interfacial tensions, γ_{SF}, γ_{SL}, and γ_{LF}, as related by Young's equation (1) for vertical surface geometry. (b) Schematic diagram showing the wetting rate and spreading process on the multi-layer Ni-Pd-Au coating.

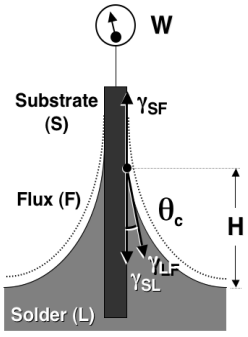

Figure 2 – Molten solder meniscus configuration from which are determined the meniscus height (H) and meniscus weight (W) using the meniscometer/wetting balance technique.

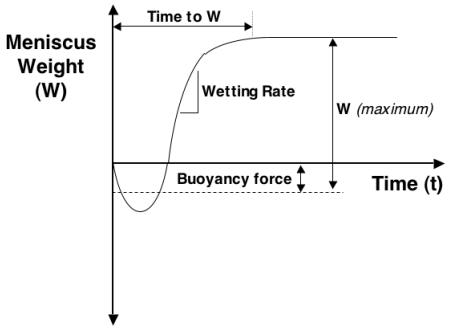

Figure 3 – Wetting balance output of meniscus weight as a function of test time. A wetting rate and wetting time are calculated from this plot.

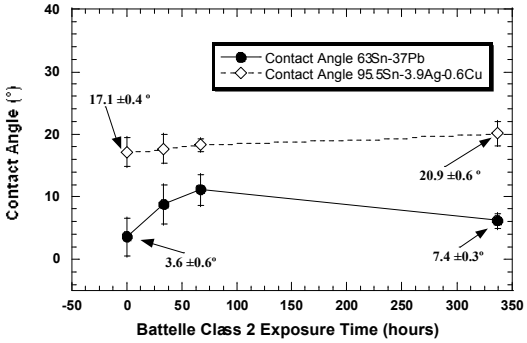

Figure 4 – The contact angle, θ_C, as a function of aging time in the Battelle Class 2 environment for the 95.5Sn-3.9Ag-0.6Cu and 63Sn-37Pb solders.

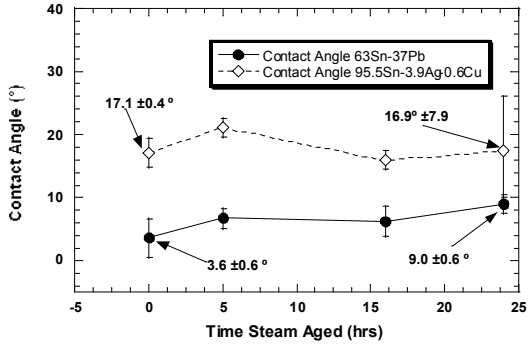

Figure 5 - The contact angle, θ_C, as a function of steam aging time interval for the 95.5Sn-3.9Ag-0.6Cu and 63Sn-37Pb solders.

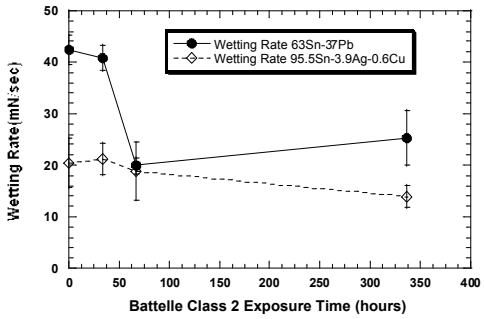

Figure 6 – The wetting rate, W_R, as a function of exposure time to the Battelle Class 2 environment for the 95.5Sn-3.9Ag-0.6Cu and 63Sn-37Pb solders.

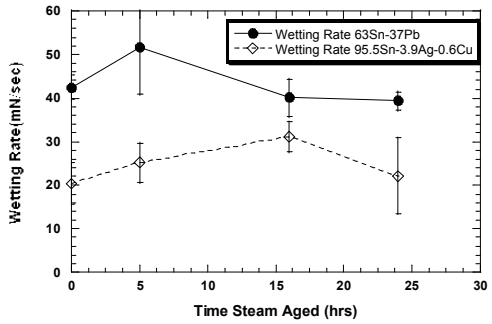

Figure 7 - The wetting rate, W_R, as a function of time after steam age for the 95.5Sn-3.9Ag-0.6Cu and 63Sn-37Pb eutectic solders.

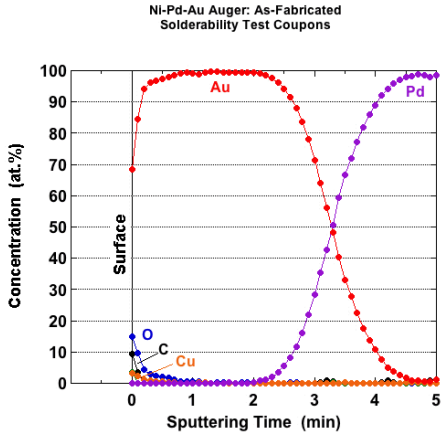

Figure 8 – Auger spectroscopy profile of Ni-Pd-Au coating in the as-fabricated condition.

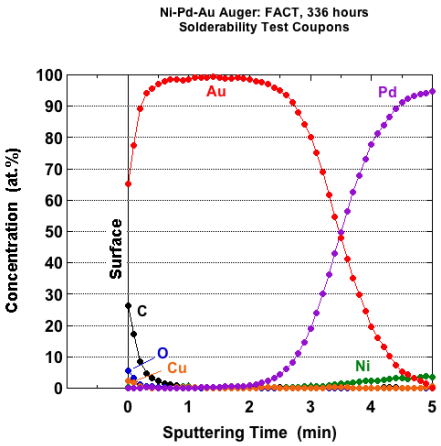

Figure 9 - Auger spectroscopy profile of Ni-Pd-Au coating after exposure to FACT for 336 hours.

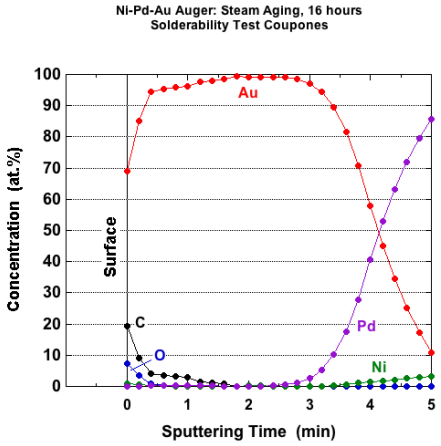

Figure 10b - Auger spectroscopy profile of Ni-Pd-Au coating after exposure to steam age for 16 hours.

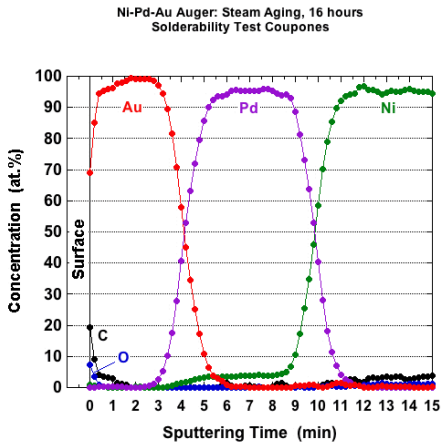

Figure 10a – Auger spectroscopy profile of Ni-Pd-Au coating after exposure to steam age for 16 hours (Elemental distributions at the longer scale into the Ni layer).